Vibrational Excitations in Single Trimetal–Molecule Transistors

ARTICLE *in* NANO LETTERS · MARCH 2006

Impact Factor: 13.59 · DOI: 10.1021/nl0519027 · Source: PubMed

6 AUTHORS, INCLUDING:

John F Berry
University of Wisconsin–Madison
99 PUBLICATIONS **2,553** CITATIONS

NANO LETTERS

2006
Vol. 6, No. 2
165−168

Vibrational Excitations in Single Trimetal-Molecule Transistors

Dong-Hun Chae,[†] John F. Berry,[‡,§] Suyong Jung,[†] F. Albert Cotton,[‡] Carlos A. Murillo,[‡] and Zhen Yao*,[†]

Department of Physics, Center for Nano- and Molecular Science and Technology, and Texas Materials Institute, The University of Texas at Austin, Austin, Texas 78712, and Laboratory for Molecular Structure and Bonding, Department of Chemistry, Texas A&M University, College Station, Texas 77843

Received September 23, 2005; Revised Manuscript Received November 29, 2005

ABSTRACT

Single-molecule transistors incorporating trimetal molecules of $Cu_3(dpa)_4Cl_2$ and $Ni_3(dpa)_4Cl_2$ (dpa = 2,2′-dipyridylamide) have been fabricated. Conductance is measured as a function of bias and gate voltages at low temperature, showing single-electron tunneling behavior through the molecules. Additional structures corresponding to the excitations in the molecules are observed, which can be attributed to intramolecular vibrational excitations coupled to the electron tunneling processes. The energies of the vibrational states are dependent on the redox state of the included molecules.

Understanding electron transport through molecules remains one of the challenges in the emerging area of molecular electronics. Recently, individual molecules have been incorporated in a transistor geometry in which the electron transport can be modulated by a gate electrode.[1−8] Transport in these devices at low temperature is dominated by single-electron tunneling[9] or the Coulomb blockade effect, which has provided a new spectroscopic tool for investigating the electronic and vibrational states at the level of individual molecules. These measurements have revealed a number of interesting phenomena including strong coupling of electron transport with molecular vibrational excitations[1,6,8] and the Kondo effect[2,3,5,7] due to correlations between unpaired electrons in the molecules and conduction electrons in the electrodes.

Previous measurements so far have focused on conjugated organic molecules or molecules containing only one or two metal atoms. Among other intriguing candidates for molecular electronics are the compounds with linear arrays of metal atoms,[10,11] especially those having extended metal atom chains (EMACs).[12] Such molecules have also been an important subject in the fundamental research of metal−metal interactions.[13−15] A unique feature of these molecules is that by using appropriate ligands, they can be extended in length with high stability.[16] Moreover, they generally have easily accessible redox states with interesting redox properties. For example, it has been shown that metal−metal separations are strongly dependent on the redox states due to metal−metal bond formation in some molecules.[14,15] This property has led to the proposal to use these molecules as molecular switches.

In this paper, we report the fabrication and characterization of single-molecule transistors (SMTs) incorporating trinuclear dipyridylamido complexes, $Cu_3(dpa)_4Cl_2$ and $Ni_3(dpa)_4Cl_2$ (dpa = 2,2′-dipyridylamide), which represent the simplest prototypical examples of EMAC molecules. Low-energy excitations are observed in Coulomb blockade tunneling spectroscopy at 4.2 K, which can be attributed to vibrational excitations coupled to the electron tunneling processes. Several charge states can be accessed in the $Cu_3(dpa)_4Cl_2$ molecules by tuning the gate voltage. Vibrational excitations are found to evolve as a function of the charge state of the molecules, which implies a change in the nature of the metal−metal interactions upon reduction or oxidation of the molecules.

$Cu_3(dpa)_4Cl_2$ (tricopper) and $Ni_3(dpa)_4Cl_2$ (trinickel) molecules are synthesized according to established procedures.[15,17] A schematic of our SMTs is shown in Figure 1a. The devices are fabricated on oxidized silicon substrates. Aluminum gate electrodes are first fabricated by optical lithography and electron-beam evaporation at liquid nitrogen temperature and subsequently oxidized by exposure to air. Thin gold nanowires with narrow constrictions of ∼100 nm and thicknesses of ∼15 nm are patterned by electron-beam lithography on top of the aluminum gates, as shown in the

* To whom correspondence should be addressed. E-mail: yao@physics.utexas.edu.
[†] The University of Texas at Austin.
[‡] Texas A&M University.
[§] Present Address: Max-Planck Institut für Bioanorganische Chemie, Stiftstrasse 34−36, D-45470 Mülheim an der Ruhr, Germany.

10.1021/nl0519027 CCC: $33.50
Published on Web 01/04/2006

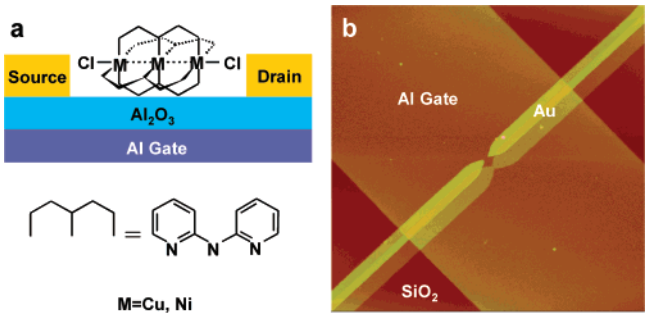

Figure 1. (a) Schematic of a single trimetal-molecule transistor. (b) An atomic force microscopic image of an Au nanobridge fabricated by electron-beam lithography and double-angle evaporation on top of Al gate electrode with a width of 5 μm.

atomic force microscope image in Figure 1b. After the nanowires are cleaned in oxygen plasma, a dilute solution (~0.2 μM) of the trimetal molecules in methanol is spin-deposited on the substrates. The samples are then cooled to 4.2 K and Au nanowires are broken via the electromigration process to create nanometer-sized gaps by ramping up a dc voltage across the wires while monitoring the resistance.[18] The breaking process is terminated when the resistance across the wires increases above ~100 kΩ. We have examined a total of 160 tricopper and 160 trinickel devices. In most devices, the breaking occurs via a series of discrete resistance steps. After breaking, these devices show either simple tunneling current with no gate dependence or no measurable current, suggesting that either no molecules are bridging the gaps or the gaps are too large. In 14 tricopper and 9 trinickel devices, the breaking process is characterized by long resistance tails, and the current−voltage ($I-V$) characteristics after breaking display voltage gaps and current steps, which can be modulated with a gate voltage. For these devices, conductance is measured in detail as a function of bias and gate voltages either by using standard ac lock-in technique or by numerically differentiating dc $I-V$ curves at different gate voltages. Among these devices, four tricopper and 7 trinickel devices show well-resolved low-energy excitations. As will be explained later, we believe that these devices are associated with the presence of molecules bridging the nanogaps.

Figure 2 shows a two-dimensional color plot of differential conductance (dI/dV) as a function of bias and gate voltages for a SMT incorporating a tricopper molecule. The conductance is suppressed around zero bias, and the size of the voltage gaps can be modulated with the application of a gate voltage. Three diamond-shaped regions can be identified in which the conductance is suppressed. There are additional bright lines running parallel to the boundaries of the blockaded regions corresponding to peaks in dI/dV.

These features are characteristic of Coulomb blockade or single-electron tunneling behavior, which occurs when the molecule is weakly coupled to the electrodes through tunneling contacts. Similar phenomena have been observed in previous SMT measurements.[1−8] In this transport regime, electrons are added to the molecule one by one as an increasingly positive gate voltage is applied. Each diamond-shaped region corresponds to a distinct redox or charge state

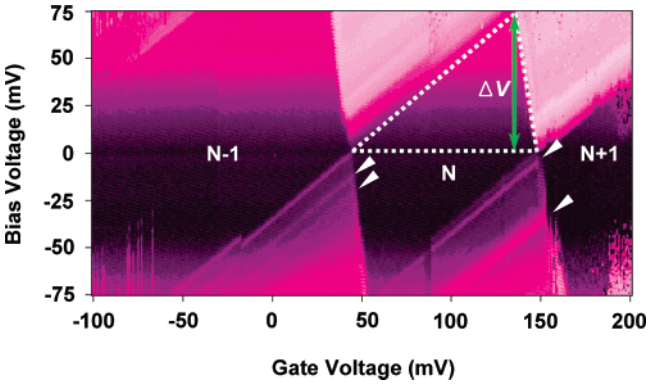

Figure 2. Color plot of dI/dV in logarithmic scale vs bias and gate voltages for a tricopper SMT measured at 4.2 K. Bright/dark colors correspond to high/low conductance. The plotted conductance ranges from 10^{-12} to 10^{-8} S. Low-energy excitations at 12.5 mV and 20.5 mV in the N electron state and at 5 mV and 33 mV in the N + 1 state are marked by arrows. This is the only device in which more than one charge degeneracy point was accessible.

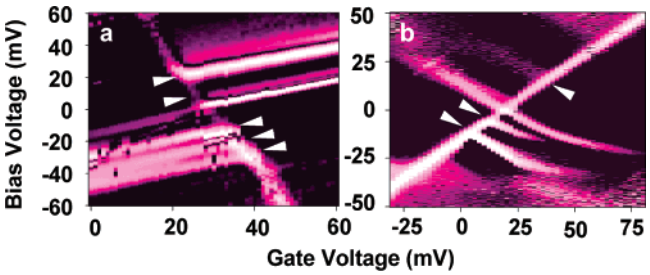

Figure 3. Color plots of dI/dV as a function of the bias and gate voltages for two different trinickel SMTs. The plotted conductance range is from 10^{-10} to 8×10^{-8} S in a and from 10^{-10} to 9×10^{-8} S in b. Excitations are marked by white arrows.

of the molecule. The initial charge state of the molecule in the absence of a gate voltage depends on the electrostatic environment and cannot be determined independently. The slopes of the boundaries of blockaded regions are determined by the capacitances of the molecule with respect to the contacts and to the gate. Thus, the observation of constant slopes for the three diamonds in Figure 2 indicates that a single molecule is bridging the gap. The voltage, ΔV, at which the boundaries of Coulomb diamonds intersect is a measure of the addition energy, which includes Coulomb charging energy and molecular energy level spacing. The plot in Figure 2 also provides a mapping of excitation energies in the molecules. A peak in dI/dV occurs whenever an excited state enters the bias voltage window, which provides an additional current pathway. The energies of the excited states in a particular charge state are obtained directly from the plot in Figure 2 as the bias voltage values at which the lines associated with the excited states intersect the boundaries of the Coulomb diamond in that charge state. For example, the arrows in the central Coulomb diamond in Figure 2 mark the excited states in the N charge state.

We have consistently observed low-energy excitations in different trimetal SMT devices. Figure 3 shows plots of differential conductance from two devices incorporating trinickel molecules. Only one charge degeneracy point was observed in these devices. The exact values of excitations

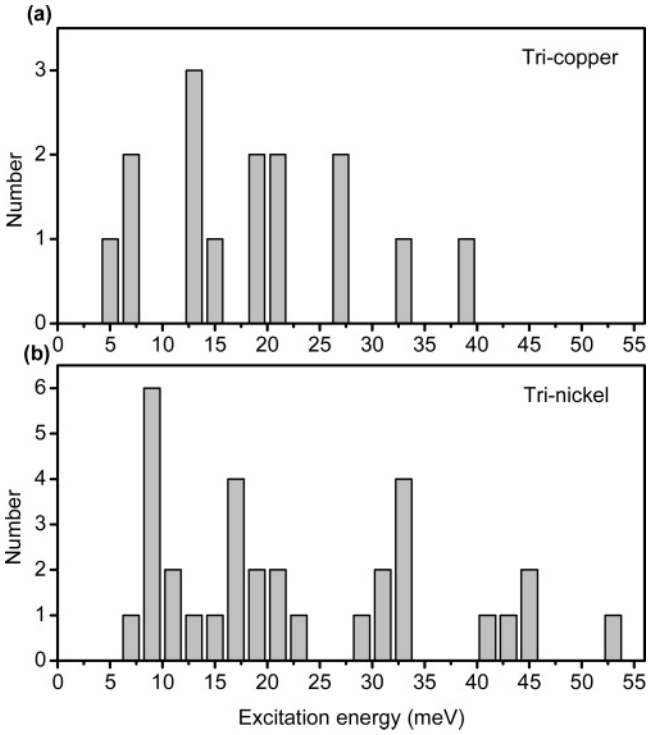

Figure 4. Histograms of observed excitations (bin = 2 meV) for (a) tricopper devices and (b) trinickel devices.

do vary from sample to sample. However, they are all on the same order of a few tens of millivolts. In Figure 4, we plot histograms of the excitation energies observed in the 4 tricopper and 7 trinickel devices.

We note that the observed addition energies of ~100 meV in Figure 2 are an order of magnitude smaller than the electronic energy level spacing obtained in solution from conventional spectroscopic measurements of trimetal molecules, which is typically a few electronvolts.[15] However, such a discrepancy was also observed previously in SMTs with conjugated oligomers and was attributed to the screening effect by image charges in the metal electrodes.[4] The addition energies observed in our molecular devices are similar to those exhibited by single-electron transistors based on Au nanoparticles, which were formed by Au evaporation between nanogaps.[19] In those devices, however, all of the Coulomb diamonds were of the same size and no excited states could be resolved in the tunneling spectroscopy at 4.2 K. We have also performed control experiments in which devices were fabricated in the same way as described above except only pure methanol was spin-coated on the substrates. Four out of a total of ~60 test devices showed gated transport with addition energies of less than 100 meV, but none of them showed any excitations in $I-V$ or dI/dV as in Figure 2 and Figure 3. These devices were presumably due to small Au nanoparticles that were nucleated in the nanogaps during electromigration. Incidentally, the formation of gold nanoparticles can probably also account for those molecular devices that did not show excited states. Taking these considerations together, we believe that the data shown in Figure 2 and Figure 3 are indeed associated with the molecules.

One common possibility for the excitations observed in Coulomb blockade measurements is electronic excitations. However, excitations of this type are unlikely to be the origin of the excitations observed in the present devices. Within the Coulomb blockade model, the difference in addition energies between adjacent Coulomb diamonds corresponds to the energy level spacing or the difference in energy level spacings. From Figure 2, the difference between the two complete diamonds is more than 50 meV, which is much larger than the 10−20 meV energy values observed in the excitation spectroscopy. Recent SMT measurements have revealed vibrational excitations as a mechanism that can couple to electronic transport.[1,8] For example, in C_{60} SMTs ~5 meV excitations were observed, consistent with center-of-mass vibrations of the molecules.[1] The molecules in the present work are of similar molecular mass to C_{60} and thus should exhibit similar center-of-mass vibrational energies assuming similar confinement potential. However, the observed excitations are larger. Moreover, if the center-of-mass vibrations are dominant, then we should see excitations of similar values in almost every device, which is not the case.

We thus attribute the excitations observed in our SMTs to internal molecular vibrations. The observed excitation energies shown in Figure 4 are in the range of those for metal−metal stretching modes in dinuclear compounds[20] studied by Raman spectroscopy. Other stretching modes such as metal-nitrogen deformations lie at higher energies. It is thus reasonable to assign the observed excitations to the internal stretching modes of the rodlike molecules even though it is probably difficult to separate pure stretches from other vibrational modes because of the complex structure of the molecules. Such modes are also expected to couple to the electron transport more strongly than other modes. To the best of our knowledge, however, internal stretches have not been identified in the vibrational spectroscopy of trimetal molecules. Nevertheless, to gain some insight into these stretching modes, we can model the trimetal molecules as three effective masses connected by two springs, each having the same effective force constant, k (Figure 5a). The effective masses are assigned as follows: m_A consists of one copper (nickel) atom, four nitrogen atoms, and one-third of total carbon and hydrogen atoms, and m_B consists of the same atoms together with an additional chlorine atom. In this model, there are two normal stretching modes along the axis: one is the symmetric (in-phase) (Figure 5b) and the other is asymmetric (out-of-phase) (Figure 5c). The ratio of the energy of the asymmetric mode, E_a, to that of symmetric mode, E_s, is given by: $E_a/E_s = \sqrt{\mu/m_B}$, where $\mu = m_A + 2m_B$ is the total mass of the molecule.[21] In the plot shown in Figure 2, two excitations can be identified clearly for the N electron charge state. If the lower excitation (12.5 meV) is assigned to the symmetric vibrational model, using the expression above, then the asymmetric vibrational energy can be estimated to be 22.7 meV, which is indeed close to the observed value, 20.5 meV, for the higher excitation.

When one more electron is added to the tricopper molecule, the excited states change significantly (Figure 2). New excitations at 5 and 33 meV appear for the N + 1

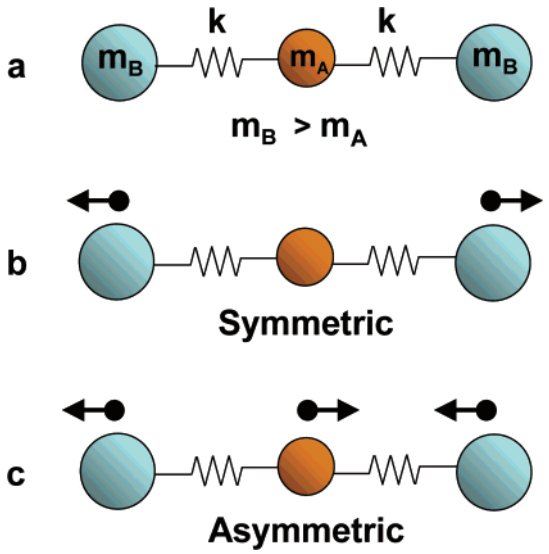

Figure 5. (a) Schematic of the mass-spring model for the trimetal molecules. Two outer masses have the same mass, m_B, and the central one has a smaller mass, m_A. b and c show the symmetric and asymmetric stretching modes along the axis.

electron state. Previous studies[15] have shown that upon oxidation or reduction metal−metal separations in trimetal molecules may change because of electrostatic interactions between metal atoms or because of formation of metal−metal bonds. The new excitations can be accounted for if we assume that the two effective force constants between metal atoms become asymmetric. However, one cannot rule out the possibility that other vibrational modes are involved, such as metal−ligand stretching, bending, or twisting deformations. A more realistic theoretical model is required in order to determine which modes couple to the electron tunneling processes most effectively.

In summary, we have fabricated SMTs incorporating trimetal EMAC complexes and observed single-electron tunneling through the molecules. Low-energy excitations have been observed consistently in tunneling spectroscopy. These features can be attributed to intramolecular stretching excitations, consistent with our simple analysis based on a mass and spring model. Furthermore, the observed vibrational excitations evolve when the charge state of the molecule is changed, highlighting the effect of metal−metal interactions upon reduction and oxidation of these compounds.

Acknowledgment. We thank the Robert A. Welch Foundation, NSF, and SPRING for support of this work.

References

(1) Park, H.; Park, J.; Lim, A. K. L.; Anderson, E. H.; Alivisatos, A. P.; McEuen, P. L. *Nature* **2000**, *407*, 57.
(2) Liang, W. J.; Shores, M. P.; Bockrath, M.; Long, J. R.; Park, H. *Nature* **2002**, *417*, 725.
(3) Park, J.; Pasupathy, A. N.; Goldsmith, J. I.; Chang, C.; Yaish, Y.; Petta, J. R.; Rinkoski, M.; Sethna, J. P.; Abruna, H. D.; McEuen, P. L.; Ralph, D. C. *Nature* **2002**, *417*, 722.
(4) Kubatkin, S.; Danilov, A.; Hjort, M.; Cornil, J.; Bredas, J. L.; Stuhr-Hansen, N.; Hedegard, P.; Bjornholm, T. *Nature* **2003**, *425*, 698.
(5) Pasupathy, A. N.; Bialczak, R. C.; Martinek, J.; Grose, J. E.; Donev, L. A. K.; McEuen, P. L.; Ralph, D. C. *Science* **2004**, *306*, 86.
(6) Yu, L. H.; Keane, Z. K.; Ciszek, J. W.; Cheng, L.; Stewart, M. P.; Tour, J. M.; Natelson, D. *Phys. Rev. Lett.* **2004**, *93*, 266802.
(7) Yu, L. H.; Natelson, D. *Nano Lett.* **2004**, *4*, 79.
(8) Pasupathy, A. N.; Park, J.; Chang, C.; Soldatov, A. V.; Lebedkin, S.; Bialczak, R. C.; Grose, J. E.; Donev, L. A. K.; Sethna, J. P.; Ralph, D. C.; McEuen, P. L. *Nano Lett.* **2005**, *5*, 203.
(9) Kouwenhoven, L. P.; Markus, C. M.; McEuen, P. L.; Tarucha, S.; Westervelt, R. M.; Wintergreen, N. S. In *Mesoscopic Electron Transport*; Kouwenhoven, L. P., Schon, G., Sohn, L. L., Eds.; Kluwer Academic Publishers: Dordrecht, The Netherlands, 1996.
(10) Bera, J. K.; Dunbar, K. R. *Angew. Chem., Int. Ed.* **2002**, *41*, 4453.
(11) Kagan, C. R.; Ratner, M. A. *MRS Bull.* **2004**, *29*, 376.
(12) Berry, J. F. In *Multiple Bonds between Metal Atoms*, 3rd ed.; Cotton, F. A., Murillo, C. A., Walton, R. A., Eds.; Springer: New York, 2005.
(13) Berry, J. F.; Cotton, F. A.; Daniels, L. M.; Murillo, C. A. *J. Am. Chem. Soc.* **2002**, *124*, 3212.
(14) Yeh, C. Y.; Chou, C. H.; Pan, K. C.; Wang, C. C.; Lee, G. H.; Su, Y. O.; Peng, S. M. *J. Chem. Soc., Dalton Trans.* **2002**, 2670.
(15) Berry, J. F.; Cotton, F. A.; Daniels, L. M.; Murillo, C. A.; Wang, X. *Inorg. Chem.* **2003**, *42*, 2418.
(16) Berry, J. F.; Cotton, F. A.; Lei, P.; Lu, T.; Murillo, C. A. *Inorg. Chem.* **2003**, *42*, 3534.
(17) Berry, J. F.; Cotton, F. A.; Lei, P.; Murillo, C. A. *Inorg. Chem.* **2003**, *42*, 377.
(18) Park, H.; Lim, A. K. L.; Alivisatos, A. P.; Park, J.; McEuen, P. L. *Appl. Phys. Lett.* **1999**, *75*, 301.
(19) Bolotin, K. I.; Kuemmeth, F.; Pasupathy, A. N.; Ralph, D. C. *Appl. Phys. Lett.* **2004**, *84*, 3154.
(20) Shriver, D. F.; Cooper, C. B. In *Advances in Infrared and Raman Spectroscopy*; Clark, R. J. H., Hester, R. E., Eds.; John Wiley: New York, 1979; Vol. 6.
(21) Landau, L. D.; Lifshitz, E. M. *Mechanics*; Pergamon Press: New York, 1976.

NL0519027